

Analytic result for the top-quark width at next-to-next-to-leading order in QCD

Long-Bin Chen,¹ Hai Tao Li,² Jian Wang,^{2,*} and Yefan Wang^{2,†}

¹*School of Physics and Materials Science, Guangzhou University, Guangzhou 510006, China*

²*School of Physics, Shandong University, Jinan, Shandong 250100, China*

We present the first full analytic results of next-to-next-to-leading order (NNLO) QCD corrections to the top-quark decay width $\Gamma(t \rightarrow Wb)$ by calculating the imaginary part of three-loop top-quark self-energy diagrams. The results are all expressed in terms of harmonic polylogarithms and valid in the whole region $0 \leq m_W^2 \leq m_t^2$. The expansions in the $m_W^2 \rightarrow 0$ and $m_W^2 \rightarrow m_t^2$ limits coincide with previous studies. Our results can also be taken as the exact prediction for the lepton invariant mass spectrum in semileptonic $b \rightarrow u$ decays. We also analytically compute the decay width including the off-shell W boson effect up to NNLO in QCD for the first time. Combining these contributions with electroweak corrections and the finite b -quark mass effect, we determine the most precise top-quark width to be 1.331 GeV for $m_t = 172.69$ GeV. The total theoretical uncertainties including those from renormalization scale choice, top-quark mass renormalization scheme, input parameters and missing higher-order corrections are scrutinized and found to be less than 1%.

Keywords: Top quark, Decay width, QCD corrections

INTRODUCTION

As the heaviest elementary particle in the standard model (SM) of particle physics, the top quark plays an important role in studies of fundamental interactions. Its properties have been investigated in great detail since its discovery at the Tevatron [1, 2]. Among them, the top-quark decay width Γ_t is one of the most important parameters. The large value of this quantity indicates that the top quark has a lifetime much shorter than the period for its hadronization [3]. Thus, we can measure directly the properties of the top quark itself, rather than the hadrons formed by top quarks. Such studies on top quarks provide an excellent playground for the precision test of the SM and the search for new physics signals.

The top quark can be produced via both strong and electroweak interactions, but decays only by electroweak interaction. In the SM, it decays almost exclusively to Wb and therefore its decay width is determined by this decay mode, i.e., $\Gamma_t = \Gamma(t \rightarrow Wb)$.

The top-quark decay width can be measured in various ways. In the first method, one could compare the shape of the reconstructed mass distribution of top quarks with samples in which the top-quark width is already known. This method relies on detector resolution and precise calibration of the jet energy scale. The missing momentum of the neutrino from top quark decay causes large uncertainties in the determination of the width. The ATLAS collaboration has measured the width to be $\Gamma_t = 1.9 \pm 0.5$ GeV using this method [4].

One may also take an indirect approach by combining the information of the branching fraction ratio $B(t \rightarrow Wb)/B(t \rightarrow Wq)$ from top-quark pair production and that of the t -channel single top-quark cross section. The CMS collaboration has performed such a measurement and determined the top-quark total decay width $\Gamma_t = 1.36 \pm 0.02$ (stat.) $^{+0.14}_{-0.11}$ (syst.) GeV [5].

Novel methods have been proposed recently. The top-quark decay width can be directly probed by measuring the on-/off-shell ratio of b -charge asymmetry from $pp \rightarrow bWj$, and a 0.2-0.3 GeV precision is expected at the high luminosity LHC [6]. Applying the same idea to the top-quark pair production, the top-quark width can be constrained with an uncertainty of 12% assuming an experimental accuracy of 5% [7]. A more realistic analysis of the ATLAS differential cross section measurement shows that a result of 1.28 ± 0.31 GeV for the width can be obtained [8].

The top-quark width can also be measured at a future e^+e^- collider. Following a multi-parameter fit approach, it can be extracted with an uncertainty of 30 MeV [9]. The sensitivity would be further improved by using polarized beams or an optimized scan strategy, and an accuracy of 21 (26) MeV can be obtained at the ILC [10] (CEPC [11]). The measurement at the CLIC will be at the same level [12].

On the theoretical side, the next-to-leading order (NLO) quantum chromodynamics (QCD) corrections to the $t \rightarrow Wb$ decay were first computed analytically in Refs. [13–15] before the discovery of the top quark. The NLO electroweak (EW) corrections were presented around the same time [16, 17]. The next-to-next-to-leading order (NNLO) QCD corrections to the top-quark decay width have been calculated in Refs. [18–21] and Ref. [22] about twenty years ago using asymptotic expansion in the $w \equiv m_W^2/m_t^2 \rightarrow 0$ and $w \rightarrow 1$ limit, respectively. Later, the total and differential decay widths were calculated numerically [23, 24], and polarized decay rates were also studied [25, 26]. Recently, the renormalization scheme and scale uncertainties in this process were discussed in [27]. However, the full analytic results of NNLO QCD corrections valid for any w from 0 to 1 are still unknown. They are helpful not only in understanding the mathematical structure of the scattering amplitude at the multiple-loop level but also in providing

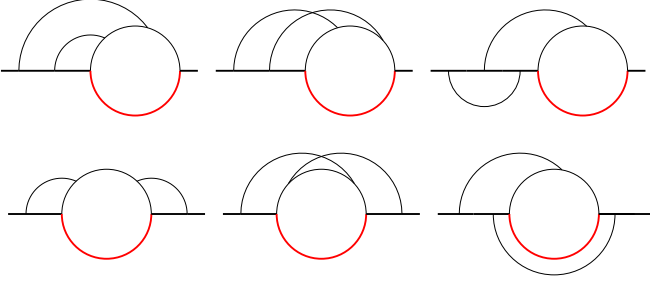


FIG. 1: The topologies of three-loop Feynman diagrams that contribute to the top-quark decay $t \rightarrow bW$ at NNLO in QCD. The thick and thin black lines stand for the top quarks and massless particles, respectively. The red lines represent the W bosons.

fast and accurate numerical results for phenomenological analyses.

CALCULATION METHODS

We calculate the top-quark decay width Γ_t by using the optical theorem to relate it to the imaginary part of top quark self-energy diagrams Σ for the process $t \rightarrow Wb \rightarrow t$,

$$\Gamma_t = \frac{\text{Im}(\Sigma)}{m_t}. \quad (1)$$

In this way, we are not bothered by the divergences that exist in the virtual and real corrections separately and the complicated phase space integration.

The amplitudes of the self-energy diagrams Σ can be generated by using the packages **FeynArts** [28] and **FeynCalc** [29]. Due to the angular momentum conservation, the final- and initial-state top quarks have the same spin. Performing summation over all the spins of the external top quarks, each amplitude is converted to a trace along the fermion line, and thus consists of scalar loop integrals. They are reduced to a minimal set of integrals called master integrals (MIs) using the identities induced from integration by parts [30, 31]. In this step, we have made use of the package **FIRE** [32]. There are nine integral families at the three-loop level. After reduction, however, we are left with six kinds of topologies, as shown in Fig. 1.

The imaginary part of Σ receives contributions from cut diagrams where some of the internal propagators can be put on-shell simultaneously [33]. In particular, the W boson propagator and at least one b quark propagator should be cut. The MIs containing such cuts are labeled cut MIs.

Then we construct canonical differential equations for the cut MIs by choosing a proper basis $\mathbf{I}(w, \epsilon)$ such that the dimensional regularisation parameter $\epsilon = (4 - d)/2$,

where d is the space-time dimension, decouples from the kinematic variables [34–36],

$$d\mathbf{I}(w, \epsilon) = \epsilon d \left[\sum_{i=1}^4 \mathbf{R}_i \log(l_i) \right] \mathbf{I}(w, \epsilon) \quad (2)$$

with the letters $l_i \in \{w-2, w-1, w, w+1\}$ and \mathbf{R}_i being rational matrices. The explicit form of the canonical basis \mathbf{I} and the differential equations in Eq. (2) are available upon request from the authors. It is highly nontrivial to achieve the canonical form for a three-loop integral basis that contains two different masses in the propagators.

In order to solve the above differential equations, boundary conditions have to be provided. Most of the basis integrals are regular at $w = 0$, i.e., they do not contain any logarithmic structure $\log(w)$, and thus can be obtained from the results for heavy-to-light decay processes [21, 37], or by using the regularity conditions of the differential equations at $w = 0$. The calculation of the basis integrals that are not regular is more technical. Some of them can be calculated directly. The others can be determined up to a constant after solving the differential equations. This constant is firstly computed numerically with an over 50-digit accuracy employing the **AMFlow** package [38, 39], and then reconstructed in analytic form using the PSLQ algorithm [40, 41].

The results of the basis integrals are all expressed in terms of multiple polylogarithms [42] with arguments l_i . In particular, we find that the letter $l_1 = w - 2$ appears always along with $w - 1$ and w . Therefore, we can change the variable $w \rightarrow 1 - w$ in those integrals containing the letter $w - 2$, making all the analytic results of the master integrals written simply in terms of harmonic polylogarithms (HPLs) as defined in [43].

Combining the cut MIs and their corresponding coefficients, we obtain analytical results for the imaginary part of three-loop top-quark self-energy diagrams, which are free of infrared divergences but still ultraviolet divergent. We then calculate the contribution of the counter-terms following the standard renormalization procedure, and find that the ultraviolet divergences cancel out exactly.

ANALYTICAL AND NUMERICAL RESULTS

The top-quark decay width for $t \rightarrow Wb$ at NNLO in QCD can be expressed as

$$\Gamma(t \rightarrow Wb) = \Gamma_0 \left[X_0 + \frac{\alpha_s}{\pi} X_1 + \left(\frac{\alpha_s}{\pi} \right)^2 X_2 \right], \quad (3)$$

where $\Gamma_0 = \frac{G_F m_t^3 |V_{tb}|^2}{8\sqrt{2}\pi}$ and the coefficients at each order of the strong coupling α_s read

$$\begin{aligned} X_0 &= (2w+1)(w-1)^2, \\ X_1 &= C_F \left(X_0 \left(-2H_{0,1}(w) + H_0(w)H_1(w) - \frac{\pi^2}{3} \right) \right) \end{aligned}$$

$$\begin{aligned}
& + \frac{1}{2}(4w+5)(w-1)^2 H_1(w) \\
& + w(2w^2 + w - 1)H_0(w) \\
& + \frac{1}{4}(6w^3 - 15w^2 + 4w + 5), \tag{4} \\
X_2 = & C_F(T_R n_l X_l + T_R n_h X_h + C_F X_F + C_A X_A).
\end{aligned}$$

Here we have taken a massless b quark for simplicity. The results for X_0 and X_1 have been well-known [13–15]. The full analytic form of X_2 is new and constitutes one of the main results of the present work. It has been decomposed in gauge-invariant color structures, which are specified in QCD by $C_F = 4/3$, $C_A = 3$, $T_R = 1/2$, and n_l (n_h) the number of massless (massive) quark species. The coefficients of each color structure at the renormalization scale $\mu = m_t$ are given by

$$\begin{aligned}
X_l = & -\frac{X_0}{3} [H_{0,1,0}(w) - H_{0,0,1}(w) - 2H_{0,1,1}(w) + 2H_{1,1,0}(w) - \pi^2 H_1(w) - 3\zeta(3)] + g_l(w), \\
X_h = & -\frac{(X_0 - 12w)}{3} [\zeta(3) - H_{0,0,1}(w)] + g_h(w), \\
X_F = & \frac{1}{12} X_0 [-6(2H_{0,1,0,1}(w) + 6H_{1,0,0,1}(w) - 3H_{1,0,1,0}(w) - 12\zeta(3)H_1(w)) - \pi^2 H_{1,0}(w)] \\
& + (X_0 + 4w) \left(-\frac{1}{6} \pi^2 H_{0,-1}(w) - 2H_{0,-1,0,1}(w) \right) \\
& + \frac{1}{12} (18w^3 - 3w^2 + 76w + 15) \pi^2 H_{0,1}(w) - \frac{1}{2} (4w^3 - 2w^2 + 4w + 3) H_{0,0,0,1}(w) \\
& + \frac{1}{2} (4w^3 - 2w^2 + 16w + 3) H_{0,0,1,0}(w) + w(2w^2 - 7w - 16) H_{0,0,1,1}(w) \\
& - \frac{1}{2} (2w^3 - 11w^2 - 28w - 1) H_{0,1,1,0}(w) + \frac{1}{720} \pi^4 (42w^3 - 191w^2 - 328w - 11) + g_F(w), \\
X_A = & \frac{1}{8} X_0 [-\pi^2 H_{1,0}(w) + 8H_{1,0,0,1}(w) - 2H_{1,0,1,0}(w) - 12\zeta(3)H_1(w)] \\
& + \frac{1}{24} (10w^3 + 33w^2 + 44w + 11) \pi^2 H_{0,1}(w) - \frac{1}{4} (8w^2 + 16w + 1) H_{0,0,0,1}(w) \\
& + (X_0 + 4w) \left(\frac{1}{12} \pi^2 H_{0,-1}(w) + H_{0,-1,0,1}(w) \right) + \frac{1}{1440} \pi^4 (86w^3 - 385w^2 - 312w + 11) \\
& - \frac{1}{4} (8w^2 + 4w + 1) (2H_{0,0,1,1}(w) - H_{0,0,1,0}(w)) + \frac{1}{4} (2w^3 + 13w^2 + 12w + 3) H_{0,1,1,0}(w) + g_A(w). \tag{5}
\end{aligned}$$

Here we have shown explicitly in each coefficient the results of maximal transcendental *weight* of HPLs, which is defined by the dimension of the vector \vec{m} in $H_{\vec{m}}(w)$. The transcendental weight can be added in each term and the ubiquitous constants π and Riemann Zeta function $\zeta(n)$ should be considered of weight one and n , respectively, since $\pi = -iH_0(-1 + i0)$ and $\zeta(n) = H_{\vec{0}_{n-1},1}(1)$. The results of lower transcendental weight are denoted by the functions $g_l(w)$, $g_h(w)$, $g_F(w)$, and $g_A(w)$, of which the explicit forms can be found in the appendix. The above results are obtained at the renormalization scale $\mu = m_t$. The scale-dependent part in these coefficients can be recovered using the fact the total decay width is scale-independent.

We have made multiple checks at various stages of the calculation. All the analytic results for the master integrals have been confirmed against the numerical **AMFlow** package [39]. The amplitudes have been calculated in two different gauges for the W boson propagator, i.e.,

the Feynman-'t Hooft gauge and the unitary gauge, and perfect agreement is found. The particles appearing in the loops and the renormalization constants are all different, and thus the agreement between the results in these two gauges provides a strong check of the correctness of our calculation. Our analytic results can be expanded to any fixed order around a w from 0 to 1. The expansion up to $\mathcal{O}(w^5)$ coincides with the result reported in [20, 21], and the expansion around $w = 1$ reproduces the asymptotic expansion result given in [22].

Though the decay width at $w = 0$ and $w = 1$ is finite, it exhibits logarithmic structures near these boundaries. We have extracted such logarithmic terms by making use of the shuffle algebra properties of the HPLs. They are shown in the appendix. It would be interesting if these logarithms could be reproduced and resummed to all orders from effective field theory.

To illustrate the difference between our exact results and the approximations in series expansions, we show the

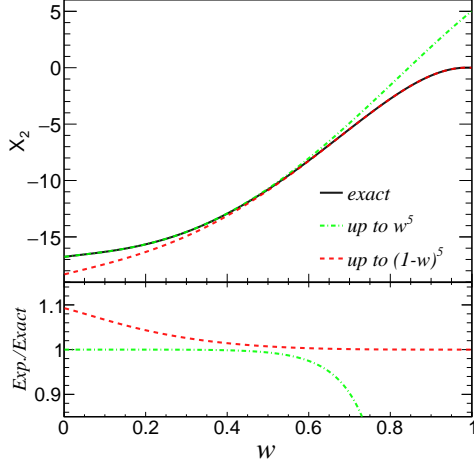


FIG. 2: Comparison between the exact result of X_2 (black line) with its expansion around $w = 0$ (dot-dashed green lines) or $w = 1$ (dashed red lines). The curves in the lower panel represent the deviation of the expansions from the exact result.

numerical values in Fig. 2. The expansion up to order w^5 , which was given explicitly in Refs. [20, 21], agrees with the exact result very well for $w < 0.5$, but begins to deviate from it for larger w . The expansion value near $w = 1$ is not approaching zero and is thus irrational, since the phase space is nearly prohibited in this region. At the other end, the difference between the series up to $(1-w)^5$, which was collected in Ref. [21], and the exact result is negligible for $w > 0.5$, but becomes sizable when w decreases. The most obvious deviation is about 10% at $w = 0$. Our analytic results unify the two expansions and are valid in the entire interval $0 \leq w \leq 1$.

The top quark decay is closely related to other important processes. Our results multiplied by a constant factor can be taken as the exact prediction for the lepton invariant mass spectrum in semileptonic $b \rightarrow u$ decays. After integration over w from 0 to 1 analytically, we reproduce the NNLO QCD correction to the total decay rate of b quark semileptonic decay $\Gamma(b \rightarrow X_u e \bar{\nu}_e)$ [44], which is a requisite to extract a precise value of the Cabibbo-Kobayashi-Maskawa matrix element V_{ub} from B meson experiments. Furthermore, if we integrate only the abelian contribution X_F over w , we obtain the analytic two-loop QED correction to the muon lifetime [45], which has been used to derive an accurate value for the Fermi coupling constant G_F [46].

In the above discussion, the W boson in the top quark decay is assumed on the mass shell. In reality, it has a width of $\Gamma_W = 2.085$ GeV [47] since it could decay immediately into leptons or quarks. After considering the fact that the top quark can decay into an off-shell

	$\delta_b^{(i)}$	$\delta_W^{(i)}$	$\delta_{EW}^{(i)}$	$\delta_{QCD}^{(i)}$	Γ_t [GeV]
LO	-0.273	-1.544	—	—	1.459
NLO	0.126	0.132	1.683	-8.575	1.361
NNLO	*	0.030	*	-2.070	1.331

TABLE I: Top-quark width up to NNLO and corrections in percentage (%) from finite b -quark mass effect, off-shell W boson contribution, EW and QCD higher orders normalized by the LO width $\Gamma_t^{(0)} = 1.486$ GeV with $m_b = 0$ and on-shell W . The values of $\delta_b^{(1)}$ and $\delta_{EW}^{(1)}$ are obtained from the formulae given in [13, 16, 48, 49]. The symbol ‘*’ denotes the contribution that has not been calculated yet. The last column gives the decay width including all the possible corrections up to that order.

W^* boson, the top-quark decay width is given by [13]

$$\begin{aligned} \tilde{\Gamma}_t &\equiv \Gamma(t \rightarrow W^* b) \\ &= \frac{1}{\pi} \int_0^{m_t^2} dq^2 \frac{m_W \Gamma_W}{(q^2 - m_W^2)^2 + m_W^2 \Gamma_W^2} \Gamma_t(q^2/m_t^2). \end{aligned} \quad (6)$$

With the analytical result of $\Gamma_t(x)$ at hand, it is straightforward to perform the integration and obtain the analytical form of $\tilde{\Gamma}_t$ in terms of multiple polylogarithms [42], which is provided in the appendix. This is another new result of our work.

Now we provide numerical results for the top-quark decay width¹. The input parameters are given by [47]

$$\begin{aligned} m_t &= 172.69 \text{ GeV}, & m_b &= 4.78 \text{ GeV}, \\ m_W &= 80.377 \text{ GeV}, & \Gamma_W &= 2.085 \text{ GeV}, \\ m_Z &= 91.1876 \text{ GeV}, & G_F &= 1.16638 \times 10^{-5} \text{ GeV}^{-2}. \end{aligned} \quad (7)$$

We choose the Cabibbo-Kobayashi-Maskawa matrix element $|V_{tb}| = 1$, and $\alpha_s(m_Z) = 0.1179$. The values of α_s at other scales are derived using the three-loop renormalization group evolution equation [50, 51]. The decay width is decomposed according to the perturbative orders,

$$\begin{aligned} \Gamma_t &= \Gamma_t^{(0)} [(1 + \delta_b^{(0)} + \delta_W^{(0)}) \\ &\quad + (\delta_b^{(1)} + \delta_W^{(1)} + \delta_{EW}^{(1)} + \delta_{QCD}^{(1)}) \\ &\quad + (\delta_b^{(2)} + \delta_W^{(2)} + \delta_{EW}^{(2)} + \delta_{QCD}^{(2)} + \delta_{EW \times QCD}^{(2)})], \end{aligned} \quad (8)$$

where the LO width $\Gamma_t^{(0)} = 1.486$ GeV with $m_b = 0$ and W on-shell, $\delta_b^{(i)}$ and $\delta_W^{(i)}$ denote the corrections from finite

¹ All the above formulae are incorporated in a Mathematica program `TopWidth` which can be downloaded from <https://github.com/haitaoli1/TopWidth>. The program has been organized in a form that can easily be used.

b quark mass effect and off-shell W boson contribution, respectively. The higher-order EW and QCD corrections are indicated by $\delta_{\text{EW}}^{(i)}$ and $\delta_{\text{QCD}}^{(i)}$, respectively. The superscripts specify the perturbative order in which they contribute.

In Table I we show their individual contributions. We can see that the dominant corrections come from QCD higher orders, which are -8.58% and -2.07% at NLO and NNLO, respectively. The NLO EW correction, calculated using the analytic expressions in [16, 49], increases the LO result by 1.68% . The off-shell W boson contributes a -1.54% correction at LO, while its effect is only 0.13% at NLO, nearly amounting to $\delta_W^{(1)} \times \delta_{\text{QCD}}^{(1)}$. The off-shell W boson effect at NNLO is further suppressed. The b quark mass correction at LO is -0.27% , as expected at the same order of m_b^2/m_t^2 . The modification at NLO is not severely suppressed compared to the LO one. We have checked that this is due to the large logarithms at subleading power. It would be interesting to investigate their structure following the method in [52].

Collecting all the contributions as shown in Table I, we obtain the top-quark width $\Gamma_t = 1.331$ GeV, which is the most precise determination of this quantity to date. When the top-quark mass varies from 170 GeV to 175 GeV, the width changes from 1.258 GeV to 1.394 GeV, displaying an almost linear dependence within this range, as shown in Fig. 3.

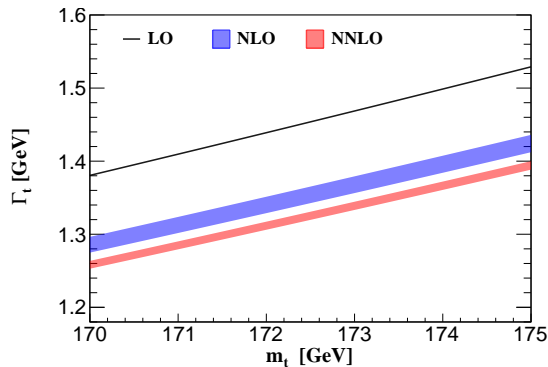


FIG. 3: Top-quark width as a function of m_t . The bands denote the QCD scale uncertainties.

Finally, we discuss the theoretical uncertainties in our results. The first uncertainty is due to the arbitrary choice of the QCD renormalization scale μ . We have chosen the default value $\mu = m_t$ in the numerical evaluation. Now we scan the scale $\mu \in [m_t/2, 2m_t]$ and find that the variation of the result is about $\pm 0.8\%$ and $\pm 0.4\%$ at NLO and NNLO, respectively, which can be seen in Fig. 3. This scale uncertainty has been reduced dramatically after including NNLO QCD corrections. The second uncertainty comes from the renormalization scheme of the top-quark mass. The top-quark mass used in Eq.

(8) is defined in the on-shell renormalization scheme. If we adopt the $\overline{\text{MS}}$ scheme in QCD corrections, the top-quark decay width would be 1.309 GeV at NLO and 1.332 GeV at NNLO, which differ from the results using the on-shell scheme by -3.79% and 0.09% at NLO and NNLO, respectively. The perturbative series using the on-shell mass usually grows rapidly at higher orders due to the infrared renormalon divergence [53]. This problem can be avoided if the decay rate is expressed in terms of the $\overline{\text{MS}}$ renormalized top-quark mass. Assuming a power-like growth for the coefficients of $(\alpha_s/\pi)^n$ [44], the missing NNNLO QCD contribution would be of the order of 0.4% . This is consistent with the expectation that the scale dependence gives a rough estimate of the unknown higher-order contributions. Third, the uncertainties at NNLO from the input parameters $\alpha_s(m_Z) = 0.1179 \pm 0.0009$ and $m_W = 80.377 \pm 0.012$ GeV [47] are 0.1% and 0.01% , respectively. Fourth, the deviation between the α scheme and the G_F scheme we have used in the EW correction is 0.1% at NLO. Lastly, the NNLO EW as well as the mixed EW \times QCD corrections have not been studied so far, but we estimate that they are of the order of $\alpha\delta_{\text{EW}}^{(1)}$ and $\delta_{\text{EW}}^{(1)} \times \delta_{\text{QCD}}^{(1)}$, respectively. Therefore, after considering all the possible uncertainties, we conclude that the uncertainty of our result at NNLO is less than 1% .

CONCLUSION

We have provided the first full analytical result of the top-quark width at NNLO in QCD. The result is obtained using the optical theorem and expressed in terms of only harmonic polylogarithms, and thus it enables a fast and exact evaluation. The off-shell W boson contribution is also calculated analytically up to NNLO in QCD for the first time. Combining our results with NLO EW corrections and finite b quark mass effects, the most precise top-quark width is predicted to be 1.331 GeV for $m_t = 172.69$ GeV with the total theoretical uncertainty less than 1% .

ACKNOWLEDGEMENTS

We would like to thank Jun Gao, Zhao Li, and Yu-Ming Wang for discussions. We thank Ansgar Denner for the communication on the implementation of the EW corrections. This work was supported in part by the National Natural Science Foundation of China under grant Nos. 12005117, 12147154, 12175048, 12275156. The work of L.B.C. was also supported by the Natural Science Foundation of Guangdong Province under grant No. 2022A1515010041. The work of J.W. was also supported by the Taishan Scholar Project of Shandong Province (tsqn201909011).

APPENDIX

The functions $g_l(w)$, $g_h(w)$, $g_F(w)$ and $g_A(w)$ in Eq.(5) are given by

$$\begin{aligned}
g_l(w) &= -\frac{(38w^2 - 55w - 37)(w-1)H_{1,0}(w)}{18} + \frac{(7w^3 - 39w^2 + 15w + 5)H_{0,1}(w)}{9} \\
&\quad - \frac{(4w+5)(w-1)^2H_{1,1}(w)}{3} + \frac{\pi^2(124w^3 - 111w^2 - 12w + 23)}{108} \\
&\quad - \frac{(124w^3 - 35w^2 - 143w + 6)(w-1)H_1(w)}{36w} - \frac{1}{36}w(106w^2 - 25w - 86)H_0(w) \\
&\quad - \frac{(99w^2 - 120w - 22)(w-1)}{36}, \\
g_h(w) &= -\frac{\pi^2(w-1)(11w^2 - 13w - 10)}{18} + \frac{(19w^4 + 32w^3 - 18w^2 - 8w + 23)\left(\frac{\pi^2}{6} - H_{0,1}(w)\right)}{9(w-1)} \\
&\quad + \frac{(265w^4 + 168w^3 - 498w^2 + 344w + 9)H_1(w)}{54w} + \frac{15902w^3 - 9237w^2 - 12528w + 12775}{1296}, \\
g_F(w) &= -\frac{1}{96}(w^2 - 12)(24H_{-1,0,0}(1-w) + 24H_{-1,0,1}(1-w) + 14\pi^2H_{-1}(1-w) - 3\zeta(3)) \\
&\quad - 18\pi^2\log(2) + (5w^2 + 8w + 3)(w-1)\left(2H_{-1,0,1}(w) + \frac{1}{6}\pi^2H_{-1}(w)\right) \\
&\quad + \frac{1}{2}(w^2 - 25w - 26)(w-1)H_{1,1,0}(w) - \frac{1}{2}(18w^3 - 9w^2 - 4w + 3)H_{0,0,1}(w) \\
&\quad + \frac{1}{4}(2w^3 - 15w^2 + 10w + 12)H_{0,1,0}(w) + \frac{1}{4}(4w^3 + 57w^2 + 4w - 54)H_{0,1,1}(w) \\
&\quad + \frac{3}{2}(w-1)^2H_{1,0,1}(w) - \frac{1}{12}\pi^2(15w^2 + 66w + 37)(w-1)H_1(w) \\
&\quad + \frac{1}{48}\pi^2w(16w^2 - 13w + 4)H_0(w) + \frac{1}{32}(400w^3 + 199w^2 - 192w - 212)\zeta(3) \\
&\quad - \frac{1}{16}\pi^2(16w^3 + 27w^2 - 76)\log(2) + \frac{1}{16}(w-1)(177w^2 - 106w - 86) \\
&\quad - \frac{(29w^2 + 24w - 1)(w-1)^2H_{1,1}(w)}{4w} + \frac{(22w^3 - 99w^2 - 63w - 2)(w-1)H_{1,0}(w)}{8w} \\
&\quad - \frac{(80w^4 - 159w^3 - 220w^2 + w + 2)H_{0,1}(w)}{8w} - \frac{1}{48}\pi^2(120w^3 + 177w^2 - 120w + 119) \\
&\quad + \frac{1}{16}(8w^3 - 385w^2 - 196w - 4)H_0(w) + \frac{(w-1)(34w^3 - 449w^2 - 175w - 2)H_1(w)}{16w}, \\
g_A(w) &= \frac{1}{192}(w^2 - 12)(24H_{-1,0,0}(1-w) + 24H_{-1,0,1}(1-w) + 14\pi^2H_{-1}(1-w) - 3\zeta(3)) \\
&\quad - 18\pi^2\log(2) + (w-1)(5w^2 + 8w + 3)\left(-H_{-1,0,1}(w) - \frac{1}{12}\pi^2H_{-1}(w)\right) + \frac{X_0}{2}H_{1,0,1}(w) \\
&\quad + \frac{1}{6}(16w^3 + 27w^2 - 24w - 13)H_{0,0,1}(w) + \frac{1}{24}(38w^3 - 117w^2 + 42w + 34)H_{0,1,0}(w) \\
&\quad - \frac{1}{24}(124w^3 - 231w^2 + 72w + 68)H_{0,1,1}(w) + \frac{1}{12}(w-1)(41w^2 - 73w - 22)H_{1,1,0}(w) \\
&\quad - \frac{1}{32}\pi^2w(16w^2 + w - 4)H_0(w) - \frac{1}{24}\pi^2(w-1)(57w^2 + 45w - 16)H_1(w) \\
&\quad - \frac{1}{64}(560w^3 - 425w^2 - 96w - 36)\zeta(3) + \frac{1}{32}\pi^2(16w^3 + 27w^2 - 76)\log(2) \\
&\quad + \frac{1}{72}(466w^2 - 827w - 485)(w-1)H_{1,0}(w) + \frac{1}{72}(32w^3 + 759w^2 + 354w - 224)H_{0,1}(w) \\
&\quad + \frac{1}{24}(166w + 65)(w-1)^2H_{1,1}(w) - \frac{1}{864}\pi^2(2614w^3 + 1005w^2 - 1272w - 505)
\end{aligned}$$

$$\begin{aligned}
& + \frac{1}{288} w (2542w^2 - 2317w - 2420) H_0(w) + \frac{(w-1)(1352w^3 - 1387w^2 - 1873w + 66) H_1(w)}{144w} \\
& + \frac{1}{576} (w-1) (1188w^2 - 3381w - 785).
\end{aligned} \tag{9}$$

Near the $w = 0$ and $w = 1$ boundaries, the decay width contains logarithmic terms. Near $w = 0$, we find

$$\begin{aligned}
X_l = & \ln(w) \left(-\frac{1}{3} (2w+1)(w-1)^2 (H_{0,1}(w) + 2H_{1,1}(w)) - \frac{1}{18} (38w^3 - 93w^2 + 18w + 37) H_1(w) \right. \\
& \left. + \frac{1}{36} w (-106w^2 + 25w + 86) \right) + \dots,
\end{aligned} \tag{10}$$

$$\begin{aligned}
X_F = & \ln(w) \left(\frac{1}{4} (w^2 - 12) H_{-1,0}(1-w) + \frac{1}{4} (2w^3 - 15w^2 + 10w + 12) H_{0,1}(w) + \frac{1}{2} (w^3 - 26w^2 - w + 26) H_{1,1}(w) \right. \\
& + \left(2w^3 - w^2 + 8w + \frac{3}{2} \right) H_{0,0,1}(w) + \frac{1}{2} (-2w^3 + 11w^2 + 28w + 1) H_{0,1,1}(w) + \frac{3}{2} (w-1)^2 (2w+1) H_{1,0,1}(w) \\
& - \frac{(w-1)((4\pi^2 - 66)w^3 + (297 - 2\pi^2)w^2 + (189 - 2\pi^2)w + 6) H_1(w)}{24w} + \frac{1}{12} \pi^2 (4w^3 - 3w^2 + w - 3) \\
& \left. + \frac{w^3}{2} - \frac{385w^2}{16} - \frac{49w}{4} - \frac{1}{4} \right) + \dots,
\end{aligned} \tag{11}$$

$$\begin{aligned}
X_A = & \ln(w) \left(-\frac{1}{8} (w^2 - 12) H_{-1,0}(1-w) + \frac{1}{24} (38w^3 - 117w^2 + 42w + 34) H_{0,1}(w) \right. \\
& + \frac{1}{12} (41w^3 - 114w^2 + 51w + 22) H_{1,1}(w) \\
& + \left(2w^2 + w + \frac{1}{4} \right) H_{0,0,1}(w) + \frac{1}{4} (2w^3 + 13w^2 + 12w + 3) H_{0,1,1}(w) - \frac{1}{4} (w-1)^2 (2w+1) H_{1,0,1}(w) \\
& - \frac{1}{72} (w-1) (-466w^2 + 9\pi^2 (2w^2 - w - 1) + 827w + 485) H_1(w) - \frac{1}{24} \pi^2 (12w^3 + w^2 - 3w - 3) \\
& \left. + \frac{1271w^3}{144} - \frac{2317w^2}{288} - \frac{605w}{72} \right) + \dots,
\end{aligned} \tag{12}$$

where the omitted parts do not contain any logarithms. X_h does not have $\ln(w)$ terms.

Near $w = 1$, we discover the logarithmic structures,

$$\begin{aligned}
X_l = & \frac{\ln^2(1-w)}{6} (w-1)^2 ((4w+2)H_0(w) - 4w - 5) \\
& + \frac{1}{36} \ln(1-w) \left(-12(2w+1)(w-1)^2 H_{0,0}(w) + 24(2w+1)(w-1)^2 H_{1,0}(w) \right. \\
& - 4(7w^3 - 39w^2 + 15w + 5) H_0(w) + \frac{(124w^3 - 35w^2 - 143w + 6)(w-1)}{w} - 12\pi^2 (2w+1)(w-1)^2 \Big) \\
& + \dots,
\end{aligned} \tag{13}$$

$$\begin{aligned}
X_h = & \frac{1}{54} \ln(1-w) \left(-18(2w^3 - 3w^2 - 12w + 1) H_{0,0}(w) + \frac{6(19w^4 + 32w^3 - 18w^2 - 8w + 23) H_0(w)}{w-1} \right. \\
& \left. - 265w^3 - 168w^2 + 498w - \frac{9}{w} - 344 \right) + \dots,
\end{aligned} \tag{14}$$

$$\begin{aligned}
X_F = & \frac{1}{8} \ln^2(1-w) \left(- (w^2 - 12) (H_{-1}(1-w) - \log(2)) + 4(2w^2 - 7w - 16) w H_{0,0}(w) \right. \\
& \left. + (4w^3 + 57w^2 + 4w - 54) H_0(w) - \frac{(w-1)^2 (29w^2 + 24w - 1)}{w} \right) \\
& + \frac{1}{48} \ln(1-w) \left(- (w^2 - 12) (-12H_{0,-1}(1-w) + 12\log(2)H_0(1-w) + \pi^2) \right. \\
& - 96(5w^2 + 8w + 3)(w-1)H_{-1,0}(w) + 24(18w^3 - 9w^2 - 4w + 3)H_{0,0}(w) \\
& \left. + 12(4w^3 + 57w^2 + 4w - 54)H_{1,0}(w) + 96(2w^3 - 3w^2 + 4w + 1)H_{0,-1,0}(w) \right)
\end{aligned}$$

$$\begin{aligned}
& +24(4w^3 - 2w^2 + 4w + 3)H_{0,0,0}(w) - 48w(2w^2 - 7w - 16)(-H_{0,1,0}(w) - H_{1,0,0}(w)) \\
& +48(2w+1)(w-1)^2H_{0,1,0}(w) + 144(2w+1)(w-1)^2H_{1,0,0}(w) - 4\pi^2(18w^3 - 3w^2 + 76w + 15)H_0(w) \\
& + \frac{6(80w^4 - 159w^3 - 220w^2 + w + 2)H_0(w)}{w} + 4\pi^2(15w^2 + 66w + 37)(w-1) - 72(w-1)^2H_{1,0}(w) \\
& - \frac{3(34w^3 - 449w^2 - 175w - 2)(w-1)}{w} - 288(2w+1)(w-1)^2\zeta(3) \Big) + \dots, \tag{15}
\end{aligned}$$

$$\begin{aligned}
X_A = & \frac{1}{48}\ln^2(1-w) \Big(-12(8w^2 + 4w + 1)H_{0,0}(w) - (124w^3 - 231w^2 + 72w + 68)H_0(w) \\
& + 3(w^2 - 12)(H_{-1}(1-w) - \log(2)) + (166w + 65)(w-1)^2 \Big) \\
& + \frac{1}{144}\ln(1-w) \Big(144(w-1)(5w^2 + 8w + 3)H_{-1,0}(w) - 24(16w^3 + 27w^2 - 24w - 13)H_{0,0}(w) \\
& - 6(124w^3 - 231w^2 + 72w + 68)H_{1,0}(w) - 144(2w^3 - 3w^2 + 4w + 1)H_{0,-1,0}(w) \\
& + 72(8w^2 + 4w + 1)(-H_{0,1,0}(w) - H_{1,0,0}(w)) - 18(w^2 - 12) \Big(H_{0,-1}(1-w) - \log(2)H_0(1-w) - \frac{\pi^2}{12} \Big) \\
& - 72(w-1)^2(2w+1)H_{1,0}(w) - 144(w-1)^2(2w+1)H_{1,0,0}(w) - 6\pi^2(10w^3 + 33w^2 + 44w + 11)H_0(w) \\
& - 2(32w^3 + 759w^2 + 354w - 224)H_0(w) + 6\pi^2(w-1)(57w^2 + 45w - 16) + 216(w-1)^2(2w+1)\zeta(3) \\
& + 36(8w^2 + 16w + 1)H_{0,0,0}(w) - \frac{(w-1)(1352w^3 - 1387w^2 - 1873w + 66)}{w} \Big) + \dots. \tag{16}
\end{aligned}$$

The top-quark width including off-shell W boson contribution is given by

$$\tilde{\Gamma}_t = \frac{\Gamma_0}{\pi} \left[\tilde{X}_0 + \frac{\alpha_s}{\pi} C_F \tilde{X}_1 + \left(\frac{\alpha_s}{\pi} \right)^2 \tilde{X}_2 \right] \tag{17}$$

with

$$\tilde{X}_0 = 2rw(2w-1) - \frac{1}{2} \left[(2(r-i)w-i)((r-i)w+i)^2 G_{w+irw}(1) + (2(r+i)w+i)((r+i)w-i)^2 G_{w-irw}(1) \right] \tag{18}$$

and

$$\begin{aligned}
\tilde{X}_1 = & \frac{1}{24}((r-i)w+i)(4\pi^2(2(r-i)^2w^2 + irw + w + 1) - 3(6(r-i)^2w^2 + (9+9ir)w + 5))G_{w+irw}(1) \\
& + \frac{1}{24}((r+i)w-i)(4\pi^2(2(r+i)^2w^2 - irw + w + 1) - 3(6(r+i)^2w^2 + (9-9ir)w + 5))G_{w-irw}(1) \\
& - \frac{1}{2}(r+i)w(2(r+i)^2w^2 + (-1+ir)w + 1)G_{w-irw,0}(1) \\
& - \frac{1}{2}(r-i)w(2(r-i)^2w^2 + (-1-ir)w + 1)G_{w+irw,0}(1) \\
& + \frac{1}{4}(4(r-i)w-5i)((r-i)w+i)^2G_{w+irw,1}(1) + \frac{1}{4}(4(r+i)w+5i)((r+i)w-i)^2G_{w-irw,1}(1) \\
& + \frac{1}{2}(2(r-i)w-i)((r-i)w+i)^2G_{w+irw,1,0}(1) + \frac{1}{2}(2(r+i)w+i)((r+i)w-i)^2G_{w-irw,1,0}(1) \\
& - \frac{1}{2}(2(r+i)w+i)((r+i)w-i)^2G_{w-irw,0,1}(1) - \frac{1}{2}(2(r-i)w-i)((r-i)w+i)^2G_{w+irw,0,1}(1) \\
& + \pi^2 r(1-2w)w + rw(3w-5). \tag{19}
\end{aligned}$$

Here $r = \frac{\Gamma_W}{m_W}$ and $G_{a_1, a_2, \dots, a_n}(x)$ are multiple polylogarithms defined in [42]. The coefficient \tilde{X}_2 can be found in the ancillary file associated with the arXiv submission of this article, arXiv:2212.06341.

* j.wang@sdu.edu.cn

[†] wangyefan@sdu.edu.cn

- [1] D0 collaboration, S. Abachi et al., *Observation of the top quark*, *Phys. Rev. Lett.* **74** (1995) 2632–2637, [[hep-ex/9503003](#)].
- [2] CDF collaboration, F. Abe et al., *Observation of top quark production in $\bar{p}p$ collisions*, *Phys. Rev. Lett.* **74** (1995) 2626–2631, [[hep-ex/9503002](#)].
- [3] I. I. Y. Bigi, Y. L. Dokshitzer, V. A. Khoze, J. H. Kuhn and P. M. Zerwas, *Production and Decay Properties of Ultraheavy Quarks*, *Phys. Lett. B* **181** (1986) 157–163.
- [4] ATLAS collaboration, *Measurement of the top-quark decay width in top-quark pair events in the dilepton channel at $\sqrt{s} = 13$ TeV with the ATLAS detector*, .
- [5] CMS collaboration, V. Khachatryan et al., *Measurement of the ratio $\mathcal{B}(t \rightarrow Wb)/\mathcal{B}(t \rightarrow Wq)$ in pp collisions at $\sqrt{s} = 8$ TeV*, *Phys. Lett. B* **736** (2014) 33–57, [[1404.2292](#)].
- [6] P. P. Giardino and C. Zhang, *Probing the top-quark width using the charge identification of b jets*, *Phys. Rev. D* **96** (2017) 011901, [[1702.06996](#)].
- [7] A. Baskakov, E. Boos and L. Dudko, *Model independent top quark width measurement using a combination of resonant and nonresonant cross sections*, *Phys. Rev. D* **98** (2018) 116011, [[1807.11193](#)].
- [8] C. Herwig, T. Ježo and B. Nachman, *Extracting the Top-Quark Width from Nonresonant Production*, *Phys. Rev. Lett.* **122** (2019) 231803, [[1903.10519](#)].
- [9] M. Martinez and R. Miquel, *Multiparameter fits to the t anti- t threshold observables at a future e^+e^- linear collider*, *Eur. Phys. J. C* **27** (2003) 49–55, [[hep-ph/0207315](#)].
- [10] T. Horiguchi, A. Ishikawa, T. Suehara, K. Fujii, Y. Sumino, Y. Kiyo et al., *Study of top quark pair production near threshold at the ILC*, [1310.0563](#).
- [11] Z. Li, X. Sun, Y. Fang, G. Li, S. Xin, S. Wang et al., *Top quark mass measurements at the $t\bar{t}$ threshold with CEPC*, [2207.12177](#).
- [12] CLICDP collaboration, H. Abramowicz et al., *Top-Quark Physics at the CLIC Electron-Positron Linear Collider*, *JHEP* **11** (2019) 003, [[1807.02441](#)].
- [13] M. Jezabek and J. H. Kuhn, *QCD Corrections to Semileptonic Decays of Heavy Quarks*, *Nucl. Phys. B* **314** (1989) 1–6.
- [14] A. Czarnecki, *QCD corrections to the decay $t \rightarrow Wb$ in dimensional regularization*, *Phys. Lett. B* **252** (1990) 467–470.
- [15] C. S. Li, R. J. Oakes and T. C. Yuan, *QCD corrections to $t \rightarrow W^+b$* , *Phys. Rev. D* **43** (1991) 3759–3762.
- [16] A. Denner and T. Sack, *The Top width*, *Nucl. Phys. B* **358** (1991) 46–58.
- [17] G. Eilam, R. R. Mendel, R. Migneron and A. Soni, *Radiative corrections to top quark decay*, *Phys. Rev. Lett.* **66** (1991) 3105–3108.
- [18] A. Czarnecki and K. Melnikov, *Two loop QCD corrections to top quark width*, *Nucl. Phys. B* **544** (1999) 520–531, [[hep-ph/9806244](#)].
- [19] K. G. Chetyrkin, R. Harlander, T. Seidensticker and M. Steinhauser, *Second order QCD corrections to $\Gamma(t \rightarrow Wb)$* , *Phys. Rev. D* **60** (1999) 114015, [[hep-ph/9906273](#)].
- [20] I. R. Blokland, A. Czarnecki, M. Slusarczyk and F. Tkachov, *Heavy to light decays with a two loop accuracy*, *Phys. Rev. Lett.* **93** (2004) 062001, [[hep-ph/0403221](#)].
- [21] I. R. Blokland, A. Czarnecki, M. Slusarczyk and F. Tkachov, *Next-to-next-to-leading order calculations for heavy-to-light decays*, *Phys. Rev. D* **71** (2005) 054004, [[hep-ph/0503039](#)].
- [22] A. Czarnecki and K. Melnikov, *Semileptonic $b \rightarrow u$ decays: Lepton invariant mass spectrum*, *Phys. Rev. Lett.* **88** (2002) 131801, [[hep-ph/0112264](#)].
- [23] J. Gao, C. S. Li and H. X. Zhu, *Top Quark Decay at Next-to-Next-to Leading Order in QCD*, *Phys. Rev. Lett.* **110** (2013) 042001, [[1210.2808](#)].
- [24] M. Brucherseifer, F. Caola and K. Melnikov, *$\mathcal{O}(\alpha_s^2)$ corrections to fully-differential top quark decays*, *JHEP* **04** (2013) 059, [[1301.7133](#)].
- [25] A. Czarnecki, J. G. Körner and J. H. Piclum, *Helicity fractions of W bosons from top quark decays at NNLO in QCD*, *Phys. Rev. D* **81** (2010) 111503, [[1005.2625](#)].
- [26] A. Czarnecki, S. Groote, J. G. Körner and J. H. Piclum, *NNLO QCD corrections to the polarized top quark decay $t(\uparrow) \rightarrow Xb + W^+$* , *Phys. Rev. D* **97** (2018) 094008, [[1803.03658](#)].
- [27] R.-Q. Meng, S.-Q. Wang, T. Sun, C.-Q. Luo, J.-M. Shen and X.-G. Wu, *QCD improved top-quark decay at next-to-next-to-leading order*, [2202.09978](#).
- [28] T. Hahn, *Generating Feynman diagrams and amplitudes with FeynArts 3*, *Comput. Phys. Commun.* **140** (2001) 418–431, [[hep-ph/0012260](#)].
- [29] V. Shtabovenko, R. Mertig and F. Orellana, *FeynCalc 9.3: New features and improvements*, *Comput. Phys. Commun.* **256** (2020) 107478, [[2001.04407](#)].
- [30] F. V. Tkachov, *A Theorem on Analytical Calculability of Four Loop Renormalization Group Functions*, *Phys. Lett. B* **100** (1981) 65–68.
- [31] K. G. Chetyrkin and F. V. Tkachov, *Integration by Parts: The Algorithm to Calculate beta Functions in 4 Loops*, *Nucl. Phys. B* **192** (1981) 159–204.
- [32] A. V. Smirnov and F. S. Chuharev, *FIRE6: Feynman Integral REduction with Modular Arithmetic*, *Comput. Phys. Commun.* **247** (2020) 106877, [[1901.07808](#)].
- [33] R. E. Cutkosky, *Singularities and discontinuities of feynman amplitudes*, *Journal of Mathematical Physics* **1** (1960) 429–433, [<https://doi.org/10.1063/1.1703676>].
- [34] A. V. Kotikov, *Differential equations method: New technique for massive Feynman diagrams calculation*, *Phys. Lett. B* **254** (1991) 158–164.

- [35] A. V. Kotikov, *Differential equation method: The Calculation of N point Feynman diagrams*, *Phys. Lett.* **B267** (1991) 123–127.
- [36] J. M. Henn, *Multiloop integrals in dimensional regularization made simple*, *Phys. Rev. Lett.* **110** (2013) 251601, [1304.1806].
- [37] T. van Ritbergen and R. G. Stuart, *On the precise determination of the Fermi coupling constant from the muon lifetime*, *Nucl. Phys. B* **564** (2000) 343–390, [hep-ph/9904240].
- [38] X. Liu, Y.-Q. Ma and C.-Y. Wang, *A Systematic and Efficient Method to Compute Multi-loop Master Integrals*, *Phys. Lett. B* **779** (2018) 353–357, [1711.09572].
- [39] X. Liu and Y.-Q. Ma, *AMFlow: A Mathematica package for Feynman integrals computation via auxiliary mass flow*, *Comput. Phys. Commun.* **283** (2023) 108565, [2201.11669].
- [40] H. Ferguson and D. Bailey, *A polynomial time, numerically stable integer relation algorithm*, 1992.
- [41] H. Ferguson, D. Bailey and S. Arno, *Analysis of PSLQ, an integer relation finding algorithm*, *Math. Comp.* **68** (1999) 351.
- [42] A. B. Goncharov, *Multiple polylogarithms, cyclotomy and modular complexes*, *Math. Res. Lett.* **5** (1998) 497–516, [1105.2076].
- [43] E. Remiddi and J. A. M. Vermaseren, *Harmonic polylogarithms*, *Int. J. Mod. Phys. A* **15** (2000) 725–754, [hep-ph/9905237].
- [44] T. van Ritbergen, *The Second order QCD contribution to the semileptonic $b \rightarrow u$ decay rate*, *Phys. Lett. B* **454** (1999) 353–358, [hep-ph/9903226].
- [45] T. van Ritbergen and R. G. Stuart, *Complete two loop quantum electrodynamic contributions to the muon lifetime in the Fermi model*, *Phys. Rev. Lett.* **82** (1999) 488–491, [hep-ph/9808283].
- [46] MuLan collaboration, V. Tishchenko et al., *Detailed Report of the MuLan Measurement of the Positive Muon Lifetime and Determination of the Fermi Constant*, *Phys. Rev. D* **87** (2013) 052003, [1211.0960].
- [47] PARTICLE DATA GROUP collaboration, R. L. Workman et al., *Review of Particle Physics*, *PTEP* **2022** (2022) 083C01.
- [48] M. Bohm, H. Spiesberger and W. Hollik, *On the One Loop Renormalization of the Electroweak Standard Model and Its Application to Leptonic Processes*, *Fortsch. Phys.* **34** (1986) 687–751.
- [49] A. Denner and T. Sack, *The W boson width*, *Z. Phys. C* **46** (1990) 653–663.
- [50] E. Gardi, G. Grunberg and M. Karliner, *Can the QCD running coupling have a causal analyticity structure?*, *JHEP* **07** (1998) 007, [hep-ph/9806462].
- [51] A. Deur, S. J. Brodsky and G. F. de Teramond, *The QCD Running Coupling*, *Nucl. Phys.* **90** (2016) 1, [1604.08082].
- [52] M. Beneke, M. Garny, S. Jaskiewicz, J. Strohm, R. Szafron, L. Vernazza et al., *Next-to-leading power endpoint factorization and resummation for off-diagonal “gluon” thrust*, *JHEP* **07** (2022) 144, [2205.04479].
- [53] M. Beneke, *Pole mass renormalon and its ramifications*, *Eur. Phys. J. ST* **230** (2021) 2565–2579, [2108.04861].